[3] Breakwell, J. V., "Minimum impulse transfer," AIAA Preprint 63-416 (August 1963); also *AIAA Progress in Astronautics and Aeronautics: Celestial Mechanics and Astrodynamics*, edited by V. G. Szebehely (Academic Press, New York, 1964), Vol. 14, pp. 583–589.

[4] Contensou, P., "Etude theorique des trajectoires optimales dans un champ de gravitation. Application au cas d'un centre d'attraction unique," Astronaut. Acta **8**, 134–150 (1962).

[5] Deutsch, R., *Orbital Dynamics of Space Vehicles* (Prentice-Hall, Inc., Englewood Cliffs, N. J., 1963), p. 172.

[6] Bliss, G. A., *Calculus of Variations* (Open Court Publishing Co., Lasalle, Ill., 1925).

[7] Hoelker, R. F. and Silber, R., "The bi-elliptical transfer between coplanar circular orbits," *Ballistic Missiles and Space Technology* (Pergamon Press, New York, 1961), Vol. 3, pp. 164–175.

APRIL 1965 AIAA JOURNAL VOL. 3, NO. 4

Attitude Stability of Earth-Pointing Satellites

T. R. KANE*
Stanford University, Stanford, Calif.

One possible motion of an unsymmetrical rigid body in the gravitational field of a fixed particle is described as follows: the mass center of the body traces out a circular path centered at the particle; one of the body's centroidal principal axes of inertia remains normal to the plane of this orbit, and a second centroidal principal axis oscillates about the line joining the particle to the mass center of the rigid body. This investigation is concerned with the stability of such motions. It reveals that, not only the inertia properties of the body, but also the amplitude of the oscillations must be taken into account, and that the problem is essentially three-dimensional, i.e., that incorrect results are obtained when only planar motions are considered.

Introduction

EARTH-pointing satellites, i.e., satellites that always present the same, or nearly the same, face to the earth are of interest both because the moon is a satellite of this sort and because they are particularly well suited for use in space communications systems and as vehicles carrying earth observation equipment. The motion of the moon has, of course, been studied extensively. However, as this satellite differs markedly in certain respects from artificial satellites that can be constructed, such analyses as have been performed to describe the moon's behavior are not necessarily applicable to artificial bodies. For example, the stability conditions stated by Lagrange[1] and recently (independently) discussed by DeBra and Delp[2] were predicated on the assumption that attitude deviations from an "equilibrium configuration" are negligible, an assumption that may be tenable in the case of the moon, but that can be violated easily during injection into orbit of an artificial earth satellite. The stability question thus remains open.

The present paper is concerned with a problem in dynamics that has a direct bearing on this question. Specifically, a system comprised of a fixed particle P and an unsymmetrical rigid body B is considered, and stability criteria are developed for motions described as follows: the mass center P^* of B moves on a circular orbit while one of the three centroidal principal axes of B remains normal to the plane of the orbit, and a second principal axis oscillates with an amplitude θ_3^* about the line $P - P^*$. (This is a planar motion, but the analysis does *not* involve the assumption that the body is prevented from performing truly three-dimensional motions. On the contrary, the results obtained underscore the importance of taking the three-dimensional character of the problem into account.)

It is found that the stability of such motions depends both on the inertia properties of the body B and on the amplitude θ_3^*. If X_1, X_2, and X_3 are principal axes passing through the mass center of B, with X_3 normal to the orbit plane and X_1 oscillating about line $P - P^*$, and if I_1, I_2, and I_3 are the corresponding principal moments of inertia, two inertia parameters K_1 and K_2, defined as $K_1 = (I_2 - I_3)/I_1$ and $K_2 = (I_3 - I_1)/I_2$, may be used to characterize the body. Every motion of the kind under consideration can then be represented by a point in a three-dimensional space of the parameters K_1, K_2, and θ_3^*. A plane removed from such a space by choosing a particular value of θ_3^* becomes an "instability chart" when K_1 and K_2 are used as axes of a rectangular cartesian coordinate system and points representing unstable cases are identified. Figures 1 and 2 are examples of such charts; crosses designate unstable motions.

A comparison of Figs. 1 and 2 brings an important fact to light: for an amplitude as small as one degree, there

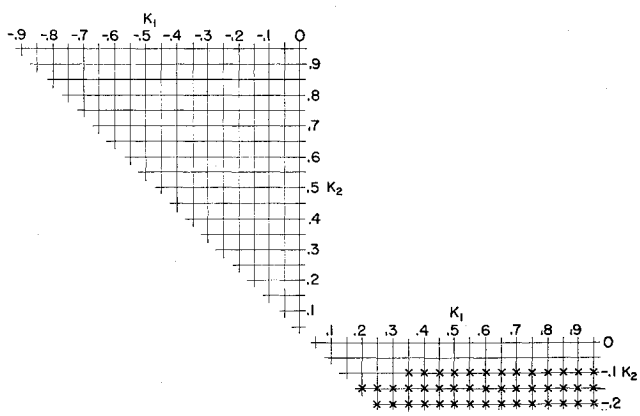

Fig. 1 Instability chart for $\theta_3^* = 0°$.

Presented as Preprint 64-657 at the AIAA/ION Astrodynamics Guidance and Control Conference, Los Angeles, Calif., August 24–26, 1964; revision received January 11, 1965. This investigation was supported, in part, under Grant NSF G-25081 of the National Science Foundation.

* Professor of Engineering Mechanics.

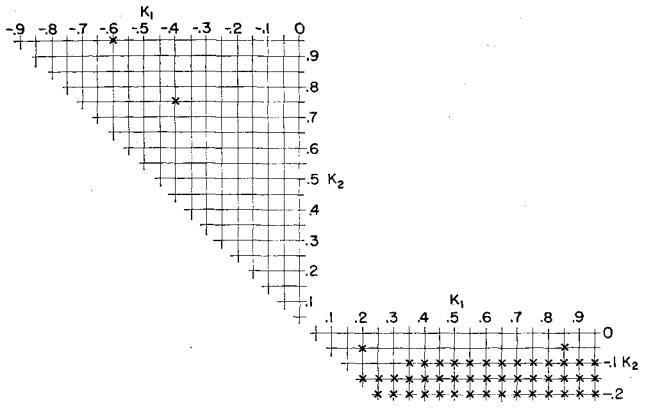

Fig. 2 Instability chart for $\theta_3^* = 1°$.

exist unstable cases that would be designated as stable if this amplitude were regarded as negligible, i.e., if Fig. 1 were used in place of Fig. 2. The applicability of the Lagrange[1] and DeBra-Delp[2] analyses to earth satellites is thus seen to be questionable.

The sequel is divided into three parts: "Dynamics," where the necessary differential equations are deduced from Newton's laws of motion and Euler's dynamical equations; "Stability," in which Floquet theory is used to establish a procedure for testing the stability of a particular motion; and "Results," dealing with the construction and interpretation of instability charts.

Dynamics

In Fig. 3, P represents a particle fixed in a Newtonian reference frame, and P^* designates the mass center of a rigid body B. Assuming that 1) the only forces affecting the motion of B significantly are those exerted on B by P, and 2) the distance between P and P^* is so large in comparison with the largest dimension of B that changes in the attitude of B have a negligible effect on the motion of P^*, one may consider motions of B during which P^* follows a circular path centered at P and having a radius R. Newton's laws of motion then require that

$$Gm/R^3 = \Omega^2 \tag{1}$$

where Ω is the (constant) "orbital angular speed," G is the universal gravitational constant, and m is the mass of P.

Let A_1, A_2, A_3 (see Fig. 3) be mutually perpendicular axes, A_2 pointing in the direction of motion of P^*, and A_3 thus being normal to the plane of the orbit. (A_1, A_2, and A_3 are sometimes called yaw, roll, and pitch axes, respectively.) Then, if X_1, X_2, X_3 are principal axes of inertia of B, the attitude of B relative to A_1, A_2, A_3 can be specified in terms of three angles θ_1, θ_2, θ_3, generated as follows: align X_i with A_i, $i = 1, 2, 3$; perform a right-handed rotation of B of amount θ_1 about A_1, bringing X_i into coincidence with B_i, $i = 1, 2, 3$ (see Fig. 4); and follow this with rotations of amount θ_2 about B_2, leading to C_1, C_2, C_3, and θ_3 about C_3, bringing B into its final position.

The angular velocity of B in inertial space, referred to the axes X_1, X_2, X_3, is given by

$$\left.\begin{aligned}
\omega_1 &= (\dot\theta_2 + \Omega\sin\theta_1)\sin\theta_3 + (\dot\theta_1\cos\theta_2 - \Omega\cos\theta_1\sin\theta_2)\cos\theta_3 \\
\omega_2 &= (\dot\theta_2 + \Omega\sin\theta_1)\cos\theta_3 - (\dot\theta_1\cos\theta_2 - \Omega\cos\theta_1\sin\theta_2)\sin\theta_3 \\
\omega_3 &= \dot\theta_1\sin\theta_2 + \Omega\cos\theta_1\cos\theta_2 + \dot\theta_3
\end{aligned}\right\} \tag{2}$$

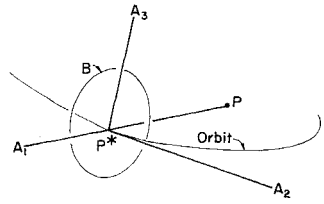

Fig. 3 Orbital reference axes.

and the gravitational torque[3] exerted on B by P, also referred to the axes X_1, X_2, X_3, is

$$\left.\begin{aligned}
M_1 &= 3(Gm/R^3)(I_2 - I_3)\sin\theta_2\cos\theta_2\sin\theta_3 \\
M_2 &= 3(Gm/R^3)(I_1 - I_3)\sin\theta_2\cos\theta_2\cos\theta_3 \\
M_3 &= 3(Gm/R^3)(I_1 - I_2)\sin\theta_3\cos\theta_3(\cos\theta_2)^2
\end{aligned}\right\} \tag{3}$$

where I_i is the moment of inertia of B about X_i, $i = 1, 2, 3$.

Before substituting from (1–3) into Euler's dynamical equations,

$$\left.\begin{aligned}
M_1 &= I_1\dot\omega_1 + (I_3 - I_2)\omega_2\omega_3 \\
M_2 &= I_2\dot\omega_2 + (I_1 - I_3)\omega_3\omega_1 \\
M_3 &= I_3\dot\omega_3 + (I_2 - I_1)\omega_1\omega_2
\end{aligned}\right\} \tag{4}$$

it is convenient to introduce a dimensionless variable τ by means of the relationship

$$\tau = \Omega t \tag{5}$$

and to define two inertia parameters K_1 and K_2 as

$$K_1 = (I_2 - I_3)/I_1 \qquad K_2 = (I_3 - I_1)/I_2 \tag{6}$$

Furthermore, to simplify the equations that follow and to facilitate some of the computations to be performed later, it is desirable to define three functions P, Q, R of θ_1, θ_2, θ_3 and of the derivatives θ_1', θ_2', θ_3' of these angles with respect to τ, as follows:

$$\left.\begin{aligned}
P &= (\sin\theta_1 + \theta_2')\cos\theta_3 + (\cos\theta_1\sin\theta_2 - \theta_1'\cos\theta_2)\sin\theta_3 \\
Q &= (\sin\theta_1 + \theta_2')\sin\theta_3 - (\cos\theta_1\sin\theta_2 - \theta_1'\cos\theta_2)\cos\theta_3 \\
R &= \cos\theta_1\cos\theta_2 + \theta_1'\sin\theta_2 + \theta_3'
\end{aligned}\right\} \tag{7}$$

Each of Eqs. (4) contains the time-derivative of one of ω_1, ω_2, ω_3. Equations (2) show that each of these quantities depends on two of the three time-derivatives $\dot\theta_1$, $\dot\theta_2$, $\dot\theta_3$. Hence, two of the quantities $\ddot\theta_1$, $\ddot\theta_2$, $\ddot\theta_3$ will occur in each of the equations obtained by substituting from (1–3) into (4). Solving the first two equations for $\ddot\theta_1$ and $\ddot\theta_2$, and eliminating t by means of Eq. (5), one finally obtains

$$\begin{aligned}
\theta_1'' = [&K_1\cos\theta_3(3\sin\theta_2\cos\theta_2\sin\theta_3 + PR) + \\
&K_2\sin\theta_3(3\sin\theta_2\cos\theta_2\cos\theta_3 - QR) - \\
&\theta_1'\sin\theta_1\sin\theta_2 + \theta_2'\cos\theta_1\cos\theta_2 - \\
&\theta_3'\sin\theta_1 + \theta_1'\theta_2'\sin\theta_2 - \theta_2'\theta_3'](\cos\theta_2)^{-1}
\end{aligned} \tag{8}$$

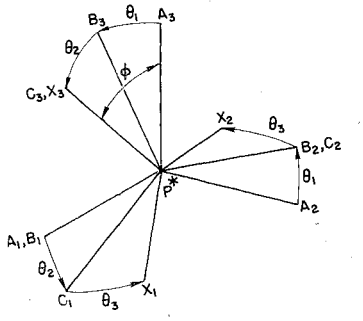

Fig. 4 Attitude angles.

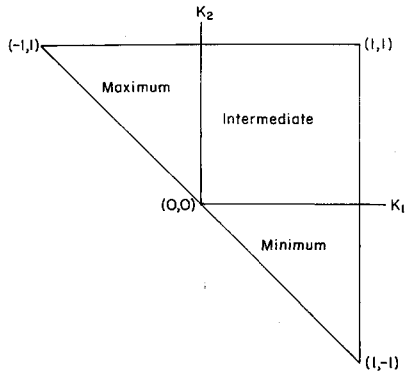

Fig. 5 Inertia parameters.

$$\theta_2'' = K_1 \sin\theta_3(3 \sin\theta_2 \cos\theta_2 \sin\theta_3 + PR) - K_2 \cos\theta_3(3 \sin\theta_2 \cos\theta_2 \cos\theta_3 - QR) - \theta_1' \cos\theta_1 - \theta_3' \cos\theta_1 \sin\theta_2 + \theta_1'\theta_3' \cos\theta_2 \quad (9)$$

$$\theta_3'' = -[(K_1 + K_2)/(1 + K_1K_2)] \times (3 \cos^2\theta_2 \sin\theta_3 \cos\theta_3 + PQ) + \theta_1' \sin\theta_1 \cos\theta_2 + \theta_2' \cos\theta_1 \sin\theta_2 - \theta_1'\theta_2' \cos\theta_2 - \theta_1'' \sin\theta_2 \quad (10)$$

These equations govern all motions of B relative to the axes A_1, A_2, A_3.

A glance at Eqs. (7–9) shows that (8) and (9) are satisfied identically if θ_1 and θ_2 are identically equal to zero, that is, whenever B moves in such a way that A_3 and X_3 (see Fig. 4) remain coincident. Equation (10) then reduces to

$$\theta_3'' + 3[(K_1 + K_2)/(1 + K_1K_2)] \sin\theta_3 \cos\theta_3 = 0 \quad (11)$$

which is, essentially, the equation of motion of a pendulum. B can thus perform motions during which X_1 oscillates about A_1 as a mean position, and the amplitude of these oscillations is completely unrestricted.

Stability

To study the stability of the oscillations described at the end of the preceding section, it is convenient to introduce a new variable θ by means of the relationship

$$\theta = 2\theta_3 \quad (12)$$

and to replace the two second-order Eqs. (8) and (9) with four first-order equations in new variables x_i, $i = 1, \ldots 4$, defined as

$$x_1 = \theta_1 \qquad x_2 = \theta_2 \qquad x_3 = \theta_1' \qquad x_4 = \theta_2' \quad (13)$$

Furthermore, as the stability of motions during which

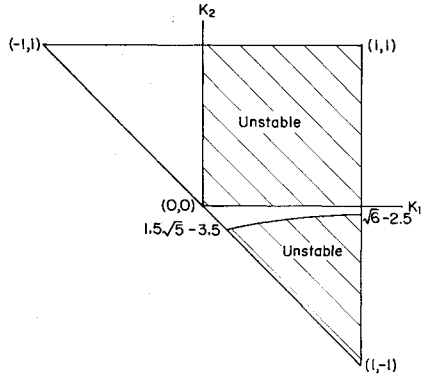

Fig. 6 Instability chart for zero amplitude.

$\theta_1 = \theta_2 = \theta_1' = \theta_2' = 0$ is to be examined, Eqs. (8–10) are linearized in $x_1, \ldots, x_4$. Equation (10) then becomes

$$\theta'' + 3[(K_1 + K_2)/(1 + K_1K_2)] \sin\theta = 0 \quad (14)$$

and Eqs. (8) and (9) lead to the four equations

$$x_i' = \sum_{j=1}^{4} w_{ij}x_j \qquad i = 1, 2, 3, 4 \quad (15)$$

where

$$w_{11} = 0 \qquad w_{12} = 0 \qquad w_{13} = 1 \qquad w_{14} = 0$$
$$w_{21} = 0 \qquad w_{22} = 0 \qquad w_{23} = 0 \qquad w_{24} = 1$$
$$w_{31} = [(2 + \theta')/4][(1 + \cos\theta)K_1 - (1 - \cos\theta)K_2] - (\theta'/2)$$
$$w_{32} = [(8 + \theta')/4](K_1 + K_2) \sin\theta$$
$$w_{33} = -[(2 + \theta')/4](K_1 + K_2) \sin\theta$$
$$w_{34} = [(2 + \theta')/4][(1 + \cos\theta)K_1 - (1 - \cos\theta)K_2] - (\theta'/2) + 1 \quad (16)$$
$$w_{41} = [(2 + \theta')/4](K_1 + K_2) \sin\theta$$
$$w_{42} = [(8 + \theta')/4][(1 - \cos\theta)K_1 - (1 + \cos\theta)K_2] - (\theta'/2)$$
$$w_{43} = -[(2 + \theta')/4][(1 - \cos\theta)K_1 - (1 + \cos\theta)K_2] + (\theta'/2) - 1$$
$$w_{44} = [(2 + \theta')/4](K_1 + K_2) \sin\theta$$

Equation (14) possesses solutions that are periodic functions of τ. The period τ^* of such a solution can be expressed in terms of the amplitude θ_3^* of the oscillations of X_1 relative to A_1 as

$$\tau^* = 4K(k)[3(K_1 + K_2)/(1 + K_1K_2)]^{-1/2} \quad (17)$$

where

$$k = \sin\theta_3^* \quad (18)$$

and $K(k)$ is the complete elliptic integral of the first kind. It follows that the coefficients w_{ij} in Eq. (15) also are periodic functions of τ of period τ^*. In accordance with Floquet theory,[4] the boundedness of the solutions of Eqs. (15) thus depends on the value at τ^* of the 4×4 matrix $H(\tau)$ defined by the matrix differential equation

$$dH(\tau)/d\tau = w(\tau)\, H(\tau) \quad (19)$$

and the initial conditions

$$H(0) = I \quad (20)$$

where $w(\tau)$ is the 4×4 matrix with w_{ij} as the element in the ith row and jth column, and I is the 4×4 unit matrix. Specifically, all solutions of Eqs. (15) are bounded as $\tau \to \infty$ if, and only if, the modulus of each of the four characteristic values of $H(\tau^*)$ is less than or equal to unity, and if, for any characteristic value λ_k such that $|\lambda_k| = 1$, the multiplicity of λ_k is equal to the nullity of the matrix $H(\tau^*) - \lambda_k I$. Given I_1, I_2 and θ_3^*, one proceeds as follows:

1) Use (6) to evaluate K_1 and K_2.
2) Find τ^* from (17) and (18).
3) Let $\theta' \equiv \theta_0'$ when $\theta = 0$, and evaluate θ_0' by noting that Eq. (14) possesses the first integral

$$(\theta')^2 = (\theta_0')^2 - 6[(K_1 + K_2)/(1 + K_1K_2)](1 - \cos\theta)$$

o that, as $\theta' = 0$ when $\theta = 2\theta_3^*$, θ_0' is given by

$$\theta_0' = \pm[12(K_1 + K_2)/(1 + K_1K_2)]^{1/2} \sin\theta_3^* \quad (21)$$

4) Perform, simultaneously, a numerical (digital computer) integration of Eq. (14) and the sixteen Eqs. (19), using for

initial values $\theta(0) = 0$, $\theta'(0) = \theta_0'$ [see Eq. (21)], and $H(0) = I$ [see Eq. (20)], and terminating the integration at $\tau = \tau^*$.

5) Find the four roots $\lambda_1, \ldots, \lambda_4$ of the characteristic equation

$$\det[H(\tau^*) - \lambda I] = 0$$

6) Determine the modulus of each distinct root.† If any one of these exceeds unity, or if it is equal to unity and the multiplicity of the corresponding root λ_k is not equal to the nullity of the matrix $H(\tau^*) - \lambda_k I$, then the motion under consideration is unstable, because Eqs. (15) then possess unbounded solutions. When these requirements for instability are not fulfilled, no conclusion is reached, because Eqs. (15) were obtained by linearization.

Results

The procedure set forth in the preceding section leads to results that, as mentioned previously, can be presented in the form of a series of plots, one for each value of θ_3^*, particular bodies being represented by points in a rectangular Cartesian coordinate system with K_1 and K_2 as axes. When constructing such a plot, it is not necessary to consider any points lying outside the triangle defined by the inequalities

$$-1 < K_i < 1 \qquad i = 1, 2 \tag{22}$$

$$K_1 + K_2 > 0 \tag{23}$$

This may be seen as follows. The sum of two principal moments of inertia always exceeds the third principal moment of inertia. Thus,

$$I_1 + I_2 > I_3 \qquad I_2 + I_3 > I_1 \qquad I_3 + I_1 > I_2 \tag{24}$$

From the first and third of these,

$$-1 < (I_2 - I_3)/I_1 < 1$$

and, from the second and first,

$$-1 < (I_3 - I_1)/I_3 < 1$$

The inequalities (22) are an immediate consequence of these relationships and of Eqs. (6). Furthermore, in view of (22), it is apparent that $1 + K_1K_2$ is an intrinsically positive quantity. Hence, Eq. (21) shows that there exists no real value of θ_0', i.e., that it is impossible to generate oscillations of amplitude θ_3^*, unless $K_1 + K_2 > 0$.

Expressed in terms of moments of inertia, the condition $K_1 + K_2 > 0$ assumes a simple and revealing form. Substitution from Eqs. (6) gives

$$I_2(I_2 - I_3) + I_1(I_3 - I_1) > 0$$

which can be expressed, alternatively, as

$$(I_2 - I_1)(I_1 + I_2 - I_3) > 0$$

or, using the first of the inequalities (24), as

$$I_1 < I_2 \tag{25}$$

The triangle defined by (22) and (23) may be subdivided into two triangular regions and one square region, as shown in Fig. 5. From (6) and (25) it follows that $I_3 > I_2 > I_1$ when $K_1 < 0$, that $I_3 < I_1 < I_2$ when $K_2 < 0$, and that $I_1 < I_3 < I_2$ when both K_1 and K_2 are positive. Thus X_3, the body-fixed axis that is normal to the orbit plane during the oscillations under consideration, is the axis of maximum or minimum centroidal moment of inertia when the body is represented by a point in the triangle in which $K_1 < 0$ or $K_1 > 0$, and points lying in the square $0 < K_1 < 1$, $0 < K_2 < 1$ correspond to bodies for which X_3 is the axis of intermediate centroidal principal moment of inertia.

† A computer program incorporating steps (1–6) was written by David J. Shippy of the University of Kentucky, Lexington, Ky. The computations were performed on an IBM 7090 computer, generously made available by the Computation Center of Stanford University.

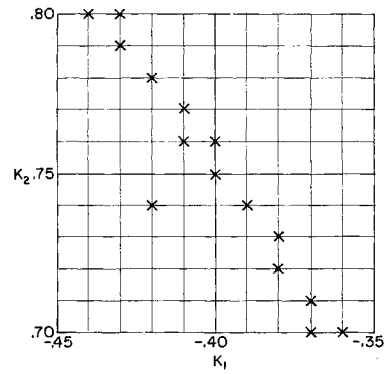

Fig. 7 Magnified portion of an instability chart.

The limiting case $\theta_3^* = 0$ can be treated in closed form and, thus, serves as a check on the procedure described in the preceding section. With $\theta = 0$, Eqs. (15) become a system of equations with constant coefficients, and the characteristic values of the matrix of the coefficients are the roots of the equation

$$\begin{vmatrix} \lambda & 0 & -1 & 0 \\ 0 & \lambda & 0 & -1 \\ -K_1 & 0 & \lambda & -(1 + K_1) \\ 0 & 4K_2 & 1 - K_2 & \lambda \end{vmatrix} = 0$$

or, in expanded form,

$$\lambda^4 + (1 + 3K_2 - K_1K_2)\lambda^2 - 4K_1K_2 = 0 \tag{26}$$

Instability is now assured when λ is real and positive, or when λ is complex, i.e., whenever one of the conditions

$$1 + 3K_2 - K_1K_2 < 0$$

$$(1 + 3K_2 - K_1K_2)^2 + 16\,K_1K_7 < 0$$

$$K_1K_2 > 0$$

is fulfilled. These become identical with "Condition III" of DeBra and Delp[2] if the inequality signs are reversed and K_1 and K_2 are replaced with k_1 and k_2, respectively; and, following these authors, one is led to the instability chart shown in Fig. 6. The corresponding chart obtained by using the procedure of the present paper is shown in Fig. 1, where each point of intersection of two lines represents a case to which the procedure was actually applied and crosses indicate instability. On this chart, as well as on all subsequent ones, detailed results are omitted both for the square $K_1 > 0$, $K_2 > 0$ and for the triangle $K_2 < -0.2$, but the computations were performed and all grid points in both regions represent unstable cases. Figs. 1 and 6 are seen to be in agreement.

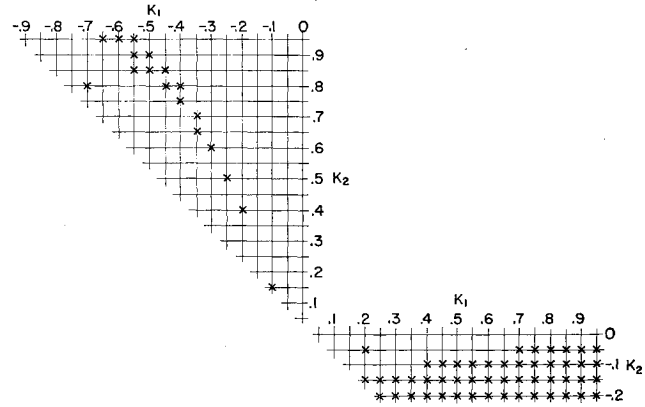

Fig. 8 Instability chart for $\theta_3^* = 5°$.

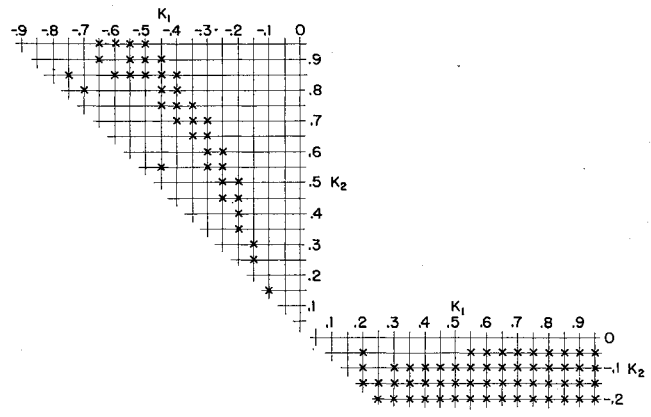

Fig. 9 Instability chart for $\theta_3^* = 10°$.

The instability chart for $\theta_3^* = 1°$, shown in Fig. 2, contains four points that indicate instabilities where none existed for $\theta_3^* = 0$. Of course, these points do not represent isolated "singularities," but are, in fact, embedded in regions of instability. In other words, if one chooses a sufficiently fine grid, one can find other points of the same character in the neighborhood of any one of these four points. For example, Fig. (7) is a magnified picture of the neighborhood of the point $K_1 = -0.4, K_2 = 0.75$.

Figure 2 must be regarded as representing a state of affairs substantially different from that described by Fig. 1 (or Fig. 6), and it is now clear that even an amplitude as small as one degree cannot be left out of account. Figures 8 and 9 illustrate the growth of zones of instability with increasing θ_3^*.

The physical significance of the instabilities here encountered can be discussed in terms of the angle ϕ between the body-fixed axis X_3 and the normal to the orbit plane A_3 (see Fig. 4). Roughly speaking, a motion during which ϕ remains small, if ϕ was initially small, is stable, whereas a motion during which ϕ grows beyond some preassigned upper limit, regardless of initial conditions, is unstable. Now, ϕ depends only on θ_1 and θ_2, and one can find these angles as functions of time (or of the number of orbits traversed by the satellite) by choosing initial values of θ_i and θ_i', $i = 1, 2, 3$, and integrating Eqs. (8–10) numerically. For example, if the body has inertia properties such that $K_1 = -0.5$ and $K_2 = 0.9$, and if $\theta_3^* = 5°$, then, with $\theta_1(0) = 0.01$, $\theta_2(0) = \theta_1'(0) = \theta_2'(0) = \theta_3(0) = 0$ and $\theta_3'(0) = 0.13$, the last being the value required by Eqs. (21) and (12), numerical integration of Eqs. (8–10), together with the relationship (see Fig. 4)

$$\phi = \arccos(\cos\theta_1 \cos\theta_2)$$

yields the plot shown in Fig. 10, which shows that ϕ reaches a maximum value of about 25 times the initial value of 0.01 rad before 20 orbits have been traversed. The question is whether or not the maximum value of ϕ can be reduced by making the initial value smaller. Figure 11 indicates what happens when $\phi(0) = 0.001$, i.e., one-tenth of the previous initial value. Nearly 30 orbits are now completed before ϕ attains a maximum, but the numerical value of this maximum remains unaltered. The integration was performed also with $\phi(0) = 10^{-6}$ and $\phi(0) = 10^{-10}$, and, in both cases, ϕ eventually attained the same maximum value as before, in the first case after about 56 orbits and in the second after about 94. This, then is a clear-cut example of instability, as it should be in view of Fig. 8, where the point $K_1 = -0.5$, $K_2 = 0.9$ is marked with a cross. By way of contrast, the nearby point $K_1 = -0.5$, $K_2 = 0.95$ of Fig. 8 gives rise to the plots shown in Figs. 12 and 13, which indicate that a reduction in ϕ at $t = 0$ now results in a proportionate reduction for all values of t, so that the maximum value of ϕ can be made arbitrarily small by an appropriate choice of $\phi(0)$.

It was stated in the Introduction that the results of the present analysis demonstrate the necessity for treating the problem of earth-pointing satellites as three-dimensional. This may be seen by examining the predictions of a solution in which the third dimension is left out of account, i.e.,

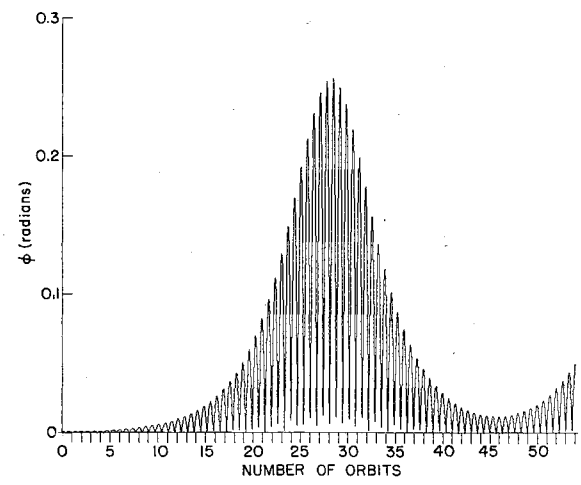

Fig. 11 $K_2 = 0.9$, $\phi(0) = 0.001$ rad.

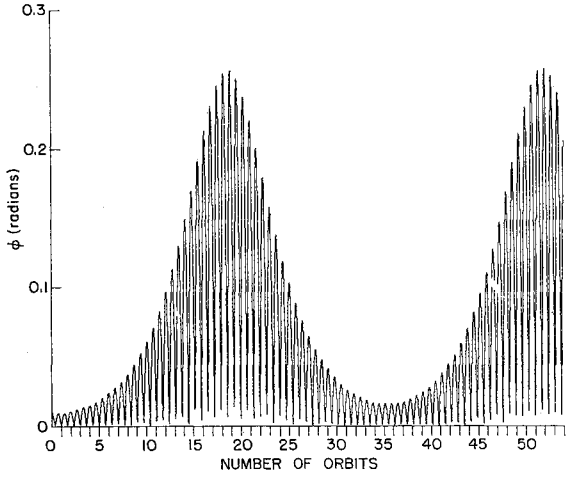

Fig. 10 $K_2 = 0.9$, $\phi(0) = 0.01$ rad.

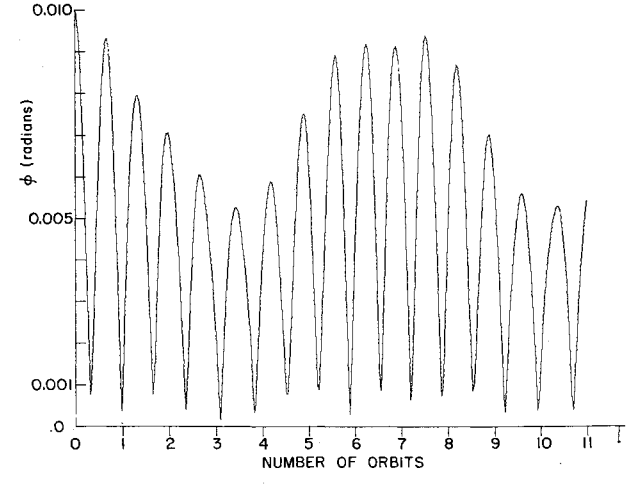

Fig. 12 $K_2 = 0.95$, $\phi(O) = 0.01$ rad.

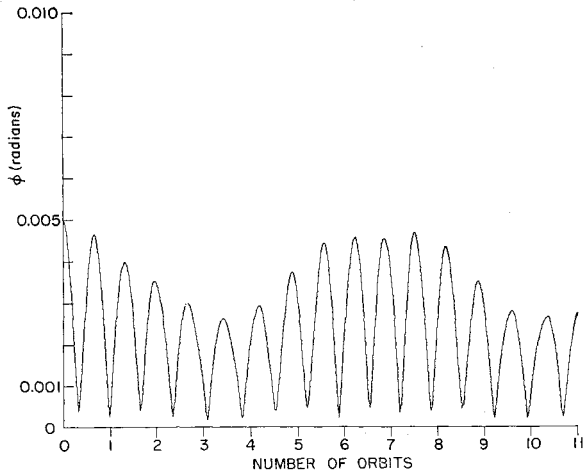

Fig. 13 $K_2 = 0.95$, $\phi(0) = 0.005$ rad.

θ_1 and θ_2 are taken identically equal to zero. All motions are then governed by Eq. (11), and the inequality (23) becomes the only stability condition. In other words, the amplitude of the body's oscillations has no bearing on the question of stability, and it must be concluded that no point in Fig. 5 represents an unstable motion, a result that conflicts with all those obtained previously. The resolution of the dilemma is simple: θ_1 and θ_2 may be taken identically equal to zero only if these angles are *physically* prevented from assuming other values, that is, if appropriate constraint forces act on the satellite. As such forces are not available in space, the problem under consideration cannot be solved by considering only planar motions.

Finally, the results here obtained show that the relationship between stability and gravitational effects is more complex than may have been supposed, and this suggests that a number of related topics, such as the one recently discussed by Garber,[5] may deserve further attention.

References

[1] Lagrange, J. L., *Oeuvres De Lagrange* (Gauthier Villars, Paris, 1870), Vol. 5, p. 97.

[2] DeBra, D. B. and Delp, R. H., "Rigid body attitude stability and natural frequencies in a circular orbit," J. Astronaut. Sci. **8**, 14–17 (1961).

[3] Plummer, H. C., *An Introductory Treatise on Dynamical Astronomy* (Dover Publications, New York, 1960), p. 294.

[4] Cesari, L., *Asymptotic Behavior and Stability Problems in Ordinary Differential Equations* (Academic Press Inc., New York, 1963), pp. 55–58.

[5] Garber, T. B., "Influence of constant disturbing torques on the motion of gravity-gradient stabilized satellites," AIAA J. **1**, 968–969 (1963).